ICASSP 2021 - 2021 IEEE International Conference on Acoustics, Speech and Signal Processing (ICASSP) | 978-1-7281-7605-5/20/$31.00 ©2021 IEEE | DOI: 10.1109/ICASSP39728.2021.9414972

ALTERNATING PROJECTIONS GRIDLESS COVARIANCE-BASED ESTIMATION FOR DOA

Yongsung Park, Peter Gerstoft

Scripps Institution of Oceanography, University of California San Diego, La Jolla, CA, 92093-0238

ABSTRACT

We present a gridless sparse iterative covariance-based estimation method based on alternating projections for direction-of-arrival (DOA) estimation. The gridless DOA estimation is formulated in the reconstruction of Toeplitz-structured low rank matrix, and is solved efficiently with alternating projections. The method improves resolution by achieving sparsity, deals with single-snapshot data and coherent arrivals, and, with co-prime arrays, estimates more DOAs than the number of sensors. We evaluate the proposed method using simulation results focusing on co-prime arrays.

Index Terms— DOA estimation, sparse signal recovery, off-grid sparse model, alternating projections, compressive sensing

1. INTRODUCTION

Direction-of-arrival (DOA) estimation is localizing several sources arriving at an array of sensors. It is an important problem in a wide range of applications, including radar, sonar, etc. Compressive sensing (CS) based DOA estimation, which promotes sparse solutions, has advantages over traditional DOA estimation methods. [1, 2] DOAs exist on a continuous angular domain, and gridless CS can be employed. [3, 4, 5] We propose a gridless sparsity-promoting DOA estimation method and apply it to co-prime arrays, which can resolve more sources than the number of sensors.

CS-based DOA estimation exploits the framework of CS, which promotes sparse solutions, for DOA estimation and has a high-resolution capability, deals with single-snapshot data, and performs well with coherent arrivals. [2, 3] To estimate DOAs in a continuous angular domain, non-linear estimation of the DOAs is linearized by using a discretized angular-search grid of potential DOAs ("steering vectors"). Grid-based CS has a basis mismatch problem [6, 7] when true DOAs do not fall on the angular-search grid. To overcome the basis mismatch, gridless CS [8, 9] has been utilized for DOA estimation. [3, 4, 5, 10, 11]

Gridless SPICE (GLS) [5, 12], one of the off-grid sparse methods, is a gridless version of sparse iterative covariance-based estimation (SPICE) [13]. GLS re-parameterizes the data covariance, or sample covariance matrix (SCM), using a positive semi-definite (PSD) Toeplitz matrix, and finds the lowest rank Toeplitz matrix which fits the SCM. The Toeplitz-structured SCM is related to a Fourier-series, which is composed of harmonics. [14, 15] GLS-based DOA estimation retrieves DOA-dependent harmonics from the SCM parameter. [5] The GLS solver uses a semi-definite programming problem (SDP), which is infeasible in practice for high-dimensional problems.

Alternating projections (AP) algorithm [16, 17] has been introduced to solve matrix completion [18, 19, 20, 21] and structured low rank matrix recovery [22, 23] and consists of projecting a matrix onto the intersection of a linear subspace and a nonconvex manifold. Atomic norm minimization (ANM) [6, 8] solves gridless CS and is equivalent to a recovery of a Toeplitz-structured low rank matrix [24]. AP based on ANM has been applied to gridless CS for DOA estimation. [25, 26]

We propose AP-based GLS for gridless CS for DOA estimation. GLS reconstructs a DOA-dependent SCM matrix, which is a Toeplitz-structured low rank matrix and has a PSD matrix in its constraint. AP-GLS solves the reconstruction of the Toeplitz-structured low rank matrix by using a sequence of projections onto the following sets: Toeplitz set, rank-constraint set, and PSD set.

Co-prime arrays are introduced for DOA estimation and offer the capability of identifying more sources than the number of sensors. [27] Sparse Bayesian learning (SBL) deals with co-prime arrays without constructing a co-array based covariance matrix and shows accurate DOAs identifying more sources than the number of sensors. [28, 29] We apply AP-GLS to co-prime arrays and show that AP-GLS with co-prime arrays estimates more DOAs than the number of sensors.

We study the performance of AP-GLS with co-prime arrays for single- and multiple-snapshot data, incoherent and coherent sources, and when the number of sources exceeds the number of sensors.

2. SIGNAL MODEL AND CO-PRIME ARRAY

2.1. Signal model

We consider K narrowband sources for L snapshot data with complex signal amplitude $s_{k,l} \in \mathbb{C}$, $k = 1, \dots, K$, $l = 1, \dots, L$. The sources have stationary DOAs for L snapshots

Supported by the Office of Naval Research, Grant No. N00014-18-1-2118.

$\theta_k \in \Theta \triangleq [-90°, 90°)$, $k = 1, \ldots, K$ in the far-field of a linear array with M sensors. The observed data $\mathbf{Y} \in \mathbb{C}^{M\times L}$ is modeled as

$$\mathbf{Y} = \sum_{k=1}^{K} \mathbf{a}(\theta_k)\mathbf{s}_{k:} + \mathbf{E} = \sum_{k=1}^{K} c_k \mathbf{a}(\theta_k)\boldsymbol{\phi}_{k:} + \mathbf{E}, \quad (1)$$

where $\mathbf{s}_{k:} = [s_{k,1} \ldots s_{k,L}] \in \mathbb{C}^{1\times L}$, $c_k = \|\mathbf{s}_{k:}\|_2 > 0$, $\boldsymbol{\phi}_{k:} = c_k^{-1}\mathbf{s}_{k:} \in \mathbb{C}^{1\times L}$ with $\|\boldsymbol{\phi}_{k:}\|_2 = 1$, $\mathbf{E} \in \mathbb{C}^{M\times L}$ is the measurement noise, and $\mathbf{a}(\theta_k) \in \mathbb{C}^M$ is the steering vector. The steering vector is given by (λ is the signal wavelength and d_m is the distance from sensor 1 to sensor m)

$$\mathbf{a}(\theta_k) = \left[1\ e^{-j\frac{2\pi}{\lambda}d_2 \sin\theta_k}\ \ldots\ e^{-j\frac{2\pi}{\lambda}d_M \sin\theta_k}\right]^{\mathsf{T}}. \quad (2)$$

2.2. Co-prime array

Consider the sensor positions in an array is given by $d_m = \delta_m d$, $m = 1, \ldots, M$, where the integer δ_m is the normalized sensor location of mth sensor and d is the minimum sensor spacing. A uniform linear array (ULA) is composed of uniformly spaced sensors with $\boldsymbol{\delta} = [0\,1 \ldots M-1]^{\mathsf{T}}$ and $d = \lambda/2$.

A co-prime array involves two ULAs with spacing $M_1 d$ and $M_2 d$ where M_1 and M_2 are co-prime, i.e., their greatest common divisor is 1. [27] A co-prime array consists of a ULA with $\boldsymbol{\delta} = [0\ M_2 \ldots (M_1-1)M_2]^{\mathsf{T}}$ and a ULA with $\boldsymbol{\delta} = [M_1\, 2M_1 \ldots (2M_2-1)M_1]^{\mathsf{T}}$, a total of M_1+2M_2-1 sensors.

We used a 16-sensor ULA with $\boldsymbol{\delta} = [0\ 1 \ldots 15]^{\mathsf{T}}$ and a 8-sensor co-prime array with $M_1 = 5$ and $M_2 = 2$, i.e., $\boldsymbol{\delta} = [0\ 2\ 4\ 5\ 6\ 8\ 10\ 15]^{\mathsf{T}}$.

3. ALTERNATING PROJECTIONS GRIDLESS SPICE

Consider the ULA case and assume incoherent sources. (GLS is robust to source correlations. [5, 12, 13]) In the noiseless case, the SCM $\mathbf{R}^* \in \mathbb{C}^{M\times M}$ is given by

$$\mathbf{R}^* = \frac{1}{L}\mathbf{Y}^*\mathbf{Y}^{*\mathsf{H}} = \sum_{k=1}^{K} p_k \mathbf{a}(\theta_k)\mathbf{a}^{\mathsf{H}}(\theta_k) \quad (3)$$

where $\mathbf{Y}^*$ is noise-free data and $p_k > 0$, $k = 1, \ldots, K$ is the power of sources, i.e., $p_k = c_k^2$. The SCM $\mathbf{R}^*$ is a (Hermitian) Toeplitz matrix,

$$\mathbf{R}^* = \mathrm{Toep}(\mathbf{r}) = \begin{bmatrix} r_1 & r_2 & \cdots & r_M \\ r_2^{\mathsf{H}} & r_1 & \cdots & r_{M-1} \\ \vdots & \vdots & \ddots & \vdots \\ r_M^{\mathsf{H}} & r_{M-1}^{\mathsf{H}} & \cdots & r_1 \end{bmatrix}, \quad (4)$$

where $\mathbf{r} \in \mathbb{C}^M$. Moreover, $\mathbf{R}^*$ is PSD and has rank K. A PSD Toeplitz matrix of rank $K < M$ can be uniquely decomposed (Vandermonde decomposition) [5, 6, 30] as

$$\mathbf{R}^* = \sum_{k=1}^{K} p_k \mathbf{a}(\theta_k)\mathbf{a}^{\mathsf{H}}(\theta_k) = \mathbf{A}\,\mathrm{diag}(\mathbf{p})\mathbf{A}^{\mathsf{H}}, \quad (5)$$

where $\mathbf{A} = [\mathbf{a}(\theta_1)\ \ldots\ \mathbf{a}(\theta_K)] \in \mathbb{C}^{M\times K}$.

GLS uses a SCM-related parameter $\mathbf{R} \in \mathbb{C}^{M\times M}$, which is a rank-$K$ PSD Toeplitz matrix, and fits the parameter $\mathbf{R}$ to SCM $\tilde{\mathbf{R}} = \mathbf{Y}\mathbf{Y}^{\mathsf{H}}/L \in \mathbb{C}^{M\times M}$. The covariance fitting is implemented, in the case of $L \geq M$ whenever $\tilde{\mathbf{R}}$ is non-singular, by minimizing the criterion, [5, 12, 13]

$$\left\|\mathbf{R}^{-\frac{1}{2}}\left(\tilde{\mathbf{R}} - \mathbf{R}\right)\tilde{\mathbf{R}}^{-\frac{1}{2}}\right\|_{\mathrm{F}}^2. \quad (6)$$

In the case of $L < M$, when $\tilde{\mathbf{R}}$ is singular, the following criterion is used instead, [5, 12]

$$\left\|\mathbf{R}^{-\frac{1}{2}}\left(\tilde{\mathbf{R}} - \mathbf{R}\right)\right\|_{\mathrm{F}}^2 = \mathrm{tr}\big(\tilde{\mathbf{R}}\mathbf{R}^{-1}\tilde{\mathbf{R}}\big) + \mathrm{tr}(\mathbf{R}) - 2\mathrm{tr}(\tilde{\mathbf{R}}). \quad (7)$$

GLS is achieved using the following optimization,

$$\begin{aligned} &\min_{\mathbf{R}}\ \mathrm{tr}\big(\tilde{\mathbf{R}}\mathbf{R}^{-1}\tilde{\mathbf{R}}\big) + \mathrm{tr}(\mathbf{R}) \quad \text{subject to}\ \ \mathbf{R} \succeq 0 \\ &\Leftrightarrow \min_{\mathbf{R},\mathbf{Z}}\ \mathrm{tr}(\mathbf{Z}) + \mathrm{tr}(\mathbf{R}) \quad \text{subject to}\ \begin{cases} \mathbf{R} \succeq 0 \\ \mathbf{Z} \succeq \tilde{\mathbf{R}}\mathbf{R}^{-1}\tilde{\mathbf{R}}, \end{cases} \\ &\Leftrightarrow \min_{\mathbf{R},\mathbf{Z}}\ \mathrm{tr}(\mathbf{Z}) + \mathrm{tr}(\mathbf{R}) \quad \text{subject to}\ \begin{bmatrix} \mathbf{R} & \tilde{\mathbf{R}} \\ \tilde{\mathbf{R}} & \mathbf{Z} \end{bmatrix} \succeq 0, \quad (8) \end{aligned}$$

where $\mathbf{R} \succeq 0$ denotes $\mathbf{R}$ is a PSD matrix and $\mathbf{Z} \in \mathbb{C}^{M\times M}$ is a free variable. Consider the case of $\mathbf{R} = \mathbf{R}^*$, then $\mathrm{tr}(\mathbf{R}) = M\sum_{k=1}^{K} p_k$. Defining $\mathrm{tr}(\mathbf{Z}) = M\sum_{k=1}^{K} p_k$, the objective in (8), divided by $2M$, equals,

$$\frac{1}{2M}\mathrm{tr}(\mathbf{R}) + \frac{1}{2M}\mathrm{tr}(\mathbf{Z}) = \sum_{k=1}^{K} p_k. \quad (9)$$

Note that, in ANM, [6, 8] minimizing $\sum_{k=1}^{K} p_k = \sum_{k=1}^{K} c_k^2$ is equivalent to minimizing the atomic norm,

$$\|\mathbf{Y}^*\|_{\mathcal{A}} = \inf_{c_k,\theta_k,\boldsymbol{\phi}_{k:}} \left\{\sum_{k=1}^{K} c_k : \mathbf{Y}^* = \sum_{k=1}^{K} c_k\,\mathbf{a}(\theta_k)\boldsymbol{\phi}_{k:}\right\}. \quad (10)$$

The atomic norm is a convex relaxation of the atomic l_0 norm, [6]

$$\|\mathbf{Y}^*\|_{\mathcal{A},0} = \inf_{c_k,\theta_k,\boldsymbol{\phi}_{k:}} \left\{K : \mathbf{Y}^* = \sum_{k=1}^{K} c_k\,\mathbf{a}(\theta_k)\boldsymbol{\phi}_{k:}\right\}. \quad (11)$$

Minimizing the atomic l_0 norm is equivalent to minimizing rank of $\mathbf{R}^* = \mathbf{Y}^*\mathbf{Y}^{*\mathsf{H}}/L$. [5, 6] Summarizing, the term $\mathrm{tr}(\mathbf{R}) = \sum_{k=1}^{K} p_k$ is the nuclear norm, used as a convex relaxation of $\mathrm{rank}(\mathbf{R})$.

By using the rank minimization in (8), the resulting optimization is as follows,

$$\min_{\mathbf{R},\mathbf{Z}}\ \mathrm{rank}(\mathbf{R}) \quad \text{subject to}\ \begin{bmatrix} \mathbf{R} & \tilde{\mathbf{R}} \\ \tilde{\mathbf{R}} & \mathbf{Z} \end{bmatrix} \succeq 0. \quad (12)$$

For the coprime array, we use the row-selection matrix $\mathbf{\Gamma}_\Omega \in \{0,1\}^{M \times M_\Omega}$, i.e.,

$$\mathbf{Y}_\Omega = \mathbf{\Gamma}_\Omega \mathbf{Y} \text{ or } \mathbf{Y} = \mathbf{\Gamma}_\Omega^\dagger \mathbf{Y}_\Omega, \tag{13}$$

where $\mathbf{Y}$ is data of full M-element ULA and the Moore-Penrose pseudo-inverse $\mathbf{\Gamma}_\Omega^\dagger$. The optimization for the coprime array is given as,

$$\min_{\mathbf{R},\mathbf{Z}} \ \operatorname{rank}(\mathbf{R}) \quad \text{subject to} \quad \begin{bmatrix} \mathbf{R}_\Omega & \tilde{\mathbf{R}}_\Omega \\ \tilde{\mathbf{R}}_\Omega & \mathbf{Z} \end{bmatrix} \succeq 0, \tag{14}$$

where $\tilde{\mathbf{R}}_\Omega = \mathbf{Y}_\Omega \mathbf{Y}_\Omega^{\mathsf{H}}/L \in \mathbb{C}^{M_\Omega \times M_\Omega}$ and $\mathbf{R}_\Omega = \mathbf{\Gamma}_\Omega \mathbf{R} \mathbf{\Gamma}_\Omega^{\mathsf{T}} \in \mathbb{C}^{M_\Omega \times M_\Omega}$. To minimize $\operatorname{rank}(\mathbf{R})$, $\mathbf{R}$ is calculated,

$$\mathbf{R} = \mathbf{\Gamma}_\Omega^\dagger \mathbf{R}_\Omega (\mathbf{\Gamma}_\Omega^\dagger)^{\mathsf{T}}. \tag{15}$$

4. ALTERNATING PROJECTIONS

We suggest alternating projections to reconstruct Toeplitz-structured low rank matrix in (12) and (14). AP-GLS involves the following sets: Toeplitz set, positive semi-definite (PSD) set, and rank-constraint set.

4.1. Projection onto the Toeplitz set

The SCM-related parameter $\mathbf{R}$ is a Toeplitz matrix, and the projection of $\mathbf{R}$ onto the Toeplitz set $\mathcal{T}$ is implemented by finding the closest Toeplitz matrix, [22, 31]

$$P_{\mathcal{T}}(\mathbf{R}) = \operatorname{Toep}(\mathbf{r}), \tag{16}$$

$$r_m = \frac{1}{2(M-m)} \sum_{i=1}^{M-m} R_{i,i+m-1} + R_{i+m-1,i}^{\mathsf{H}}. \tag{17}$$

Note that, mth component of $\mathbf{r} \in \mathbb{C}^M$ is obtained by averaging mth diagonal and the conjugate diagonal components.

4.2. Projection onto the PSD set

The constraints (12) and (14) include PSD matrices, which is obtained by projecting the matrix in the constraint onto the PSD set $\mathcal{P}$, defined by the PSD cone. The projection of a (Hermitian) matrix $\mathbf{S}$ onto the PSD set is achieved from the eigen-decomposition $\mathbf{S} = \sum_{i=1}^{2M} \mu_i \mathbf{q}_i \mathbf{q}_i^{\mathsf{H}}$, [16, 17]

$$P_{\mathcal{P}}(\mathbf{S}) = \sum_{i=1}^{2M} \max\{0, \mu_i\} \mathbf{q}_i \mathbf{q}_i^{\mathsf{H}}. \tag{18}$$

4.3. Projection onto the rank-constraint set

The objectives (12) and (14) include rank-constraints. Consider the case of rank-K matrix $\mathbf{R}$. The projection of $\mathbf{R}$ onto the rank-constraint set $\mathcal{R}$ is achieved from the singular value decomposition and taking the K-largest singular values, [19, 23]

$$P_{\mathcal{R}}(\mathbf{R}) = \sum_{k=1}^{K} \sigma_k \mathbf{u}_k \mathbf{v}_k^{\mathsf{H}}, \tag{19}$$

where σ_k, $\mathbf{u}_k \in \mathbb{C}^M$, $\mathbf{v}_k \in \mathbb{C}^M$, $k = 1, \dots, K$, are the K-largest singular values and the corresponding left and right singular vectors. We remark that $\mathbf{R}$ is an SCM, thus the eigen-decomposition and the singular value decomposition result in the same results.

Algorithm 1 AP-GLS

Input: $\mathbf{Y} \in \mathbb{C}^{M \times L}$, K, $\mathbf{\Gamma}_\Omega$
Parameters: $\epsilon_{\min} = 10^{-3}$
Initialization: $\mathbf{R} \in \mathbb{C}^{M \times M}$, $\mathbf{Z} \in \mathbb{C}^{M \times M}$ with uniformly $(0,1)$ distributed random for real and imaginary part.
$\mathbf{R}^{\text{old}} = \mathbf{R}$, $\mathbf{Z}^{\text{old}} = \mathbf{Z}$
while $\|\mathbf{S} - \mathbf{S}^{\text{old}}\|_{\text{F}} < \epsilon_{\min}$ **do**
  $\mathbf{S} = \begin{bmatrix} \mathbf{\Gamma}_\Omega \mathbf{R}^{\text{old}} \mathbf{\Gamma}_\Omega^{\mathsf{T}} & \tilde{\mathbf{R}}_\Omega \\ \tilde{\mathbf{R}}_\Omega & \mathbf{Z}^{\text{old}} \end{bmatrix}$
  PSD projection: $\mathbf{S} = P_{\mathcal{P}}(\mathbf{S})$ (18)
  $\mathbf{R} = \mathbf{\Gamma}_\Omega^\dagger \mathbf{S}(1:M, 1:M) (\mathbf{\Gamma}_\Omega^\dagger)^{\mathsf{T}}$ (15)
  Rank-constraint projection: $\mathbf{R} = P_{\mathcal{R}}(\mathbf{R})$ (19)
  Toeplitz projection: $\mathbf{R} = P_{\mathcal{T}}(\mathbf{R})$ (16)
  $\mathbf{S}(1:M, 1:M) = \mathbf{\Gamma}_\Omega \mathbf{R} \mathbf{\Gamma}_\Omega^{\mathsf{T}}$
  $\mathbf{R}^{\text{old}} = \mathbf{R}$, $\mathbf{Z}^{\text{old}} = \mathbf{S}(M+1:2M, M+1:2M)$
end while
Output: $\mathbf{R}$

4.4. Alternating projections

Initialized parameters $\mathbf{R}$ and $\mathbf{Z}$ form $\mathbf{S}$, which is PSD, i.e., $\mathbf{S} = P_{\mathcal{P}}(\mathbf{S})$ (18). $\mathbf{R}$ is obtained from $\mathbf{S}$, $\mathbf{R} = \mathbf{\Gamma}_\Omega^\dagger \mathbf{S}(1:M, 1:M)(\mathbf{\Gamma}_\Omega^\dagger)^{\mathsf{T}}$ (15), and the projection $P_{\mathcal{R}}(\mathbf{R})$ (19) is carried out to make $\mathbf{R}$ be K-rank. The projection $P_{\mathcal{T}}(\mathbf{R})$ (16) is followed for a Toeplitz structure. Submatrix $\mathbf{\Gamma}_\Omega \mathbf{R} \mathbf{\Gamma}_\Omega^{\mathsf{T}}$ is implemented in $\mathbf{S}$. AP-GLS iterates the projections until it converges to a solution. AP-GLS is summarized in Algorithm 1.

4.5. DOA retrieval

DOAs θ_k, $k = 1, \dots, K$, are recovered by the Vandermonde decomposition (5) for the rank-K PSD Toeplitz matrix $\mathbf{R}$. [5, 6, 8] The Vandermonde decomposition is computed efficiently via root-MUSIC [26]:

1. Perform the eigen-decomposition in signal- and noise-subspace, i.e., $\mathbf{R} = \mathbf{U}_S \mathbf{\Lambda}_S \mathbf{U}_S^{\mathsf{H}} + \mathbf{U}_N \mathbf{\Lambda}_N \mathbf{U}_N^{\mathsf{H}}$.
2. Compute the root-MUSIC polynomial $\mathcal{Q}(z) = \mathbf{a}^{\mathsf{T}}(1/z) \mathbf{U}_N \mathbf{U}_N^{\mathsf{H}} \mathbf{a}(z)$, where $\mathbf{a} = [1, z, \dots, z^{M-1}]^{\mathsf{T}}$ and $z = e^{-j(2\pi/\lambda) d \sin\theta}$.
3. Find the roots of $\mathcal{Q}(z)$ and choose the K roots that are inside the unit circle and closest to the unit circle, i.e., $\hat{z}_i$, $i = 1, \dots, K$.
4. DOA estimates are recovered, i.e., $\hat{\theta}_i = -\sin^{-1}(\frac{\lambda \angle \hat{z}_i}{2\pi d})$, $i = 1, \dots, K$.

5. SIMULATION RESULTS

We consider a ULA with $M = 16$ elements, half-wavelength spacing, and a co-prime array with $M = 8$ elements with $M_1 = 5$ and $M_2 = 2$ (elements 1, 3, 5, 6, 7, 9, 11, 16).

The signal-to-noise ratio (SNR) is defined, SNR $= 10 \log_{10}[\mathbb{E}\{\|\mathbf{A}\mathbf{s}_l\|\}_2^2 / \mathbb{E}\{\|\mathbf{e}_l\|\}_2^2]$, where $\mathbf{s}_l \in \mathbb{C}^K$ and $\mathbf{e}_l \in \mathbb{C}^M$, $l = 1, \dots, L$, are the source amplitude and the measurement noise for the lth snapshot. The root mean squared error

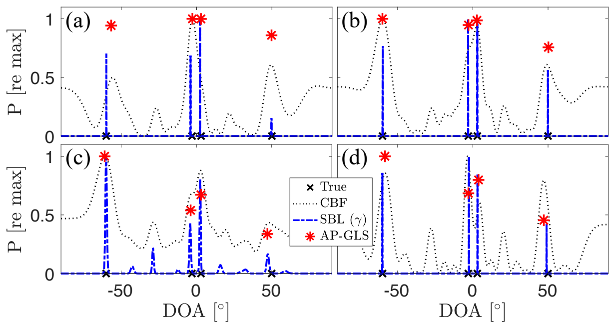

Fig. 1. DOA estimation from L snapshots for $K = 4$ sources with an $M = 8$ co-prime array. CBF, SBL, and AP-GLS for (a) incoherent sources with SNR 20 dB and one snapshot, $L = 1$, (b) SNR 20 dB and $L = 20$, (c) SNR 0 dB and $L = 20$, and (d) for coherent sources with SNR 20 dB and $L = 20$.

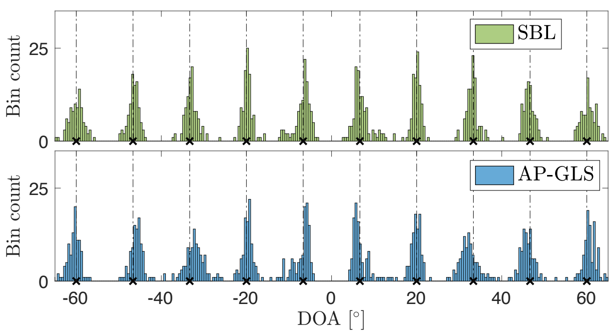

Fig. 2. Histogram of the estimated DOAs of SBL and AP-GLS for $K = 10$ sources with an $M = 8$ co-prime array for 100 trials. ($M < K$)

(RMSE) is, RMSE $= \sqrt{\mathbb{E}\left[\frac{1}{K}\sum_{k=1}^{K}\left(\hat{\theta}_k - \theta_k\right)^2\right]}$, where $\hat{\theta}_k$ and θ_k represent estimated and true DOA of the kth source.

We consider an $M = 8$ co-prime array and $K = 4$ stationary sources at DOAs $[-60, -3, 3, 50]^\circ$ with snapshot-varying magnitudes $[12, 20]$ dB in four scenarios, see Fig. 1. Conventional beamforming (CBF), SBL [28, 29], and AP-GLS are compared. CBF cannot distinguish close two DOAs $[-3, 3]^\circ$. AP-GLS solves the single snapshot case and resolve the close arrivals. We also consider the DOA performance with a coherent sources due to multipath arrivals. AP-GLS still shows accurate DOAs.

Co-prime arrays can estimate more sources than the number of sensors, see Fig. 2. We consider the same co-prime array and $K = 10$ stationary sources uniformly distributed in $[-60, 60]^\circ$, with $L = 20$ and SNR 20 dB. The histogram shows the distribution of the DOA estimates of AP-GLS.

The DOA performance is evaluated with the RMSE versus SNR, see Fig. 3. RMSE larger than 10 times the median is outlier and eliminated. We consider $K = 4$ sources, same as in Fig. 1 but with equal strengths. Cramér-Rao bound (CRB) [32], MUSIC and MUSIC with co-array interpolation (MUSIC-I) [33] are also compared. Compared to full ULA cases, AP-GLS has a bounded error even with high SNR, which is come from the fact that $\mathbf{R}$ is recovered from its submatrix $\mathbf{\Gamma}_\Omega \mathbf{R} \mathbf{\Gamma}_\Omega^\mathsf{T}$.

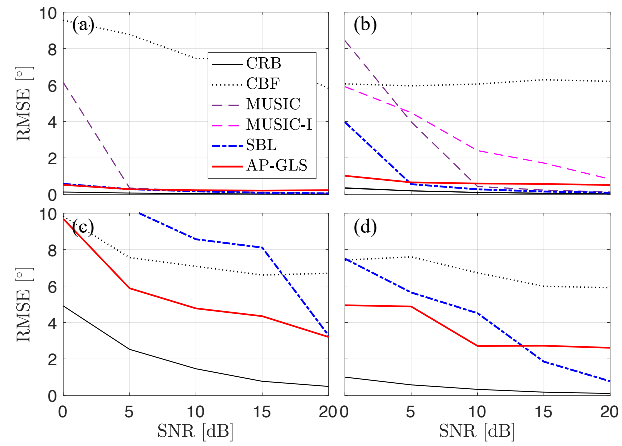

Fig. 3. RMSE [°] comparison versus SNR. Each RMSE is averaged over 100 trials. $K = 4$ incoherent sources for (a) an $M = 16$ ULA with $L = 20$, (b) an $M = 8$ co-prime array with $L = 20$, (c) $L = 1$, and (d) coherent sources for a co-prime array with $L = 20$.

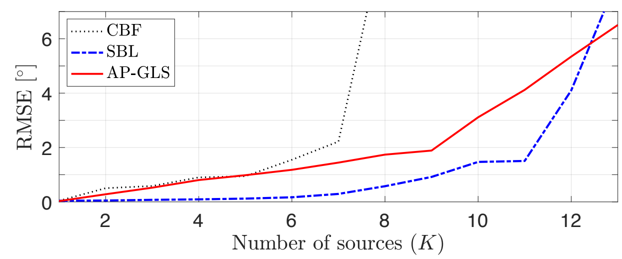

Fig. 4. RMSE [°] comparison versus K. Each RMSE is averaged over 100 trials. An $M = 8$ co-prime array is used with $L = 20$ and SNR 20 dB.

The DOA performance is evaluated with the RMSE versus number of sources K, see Fig. 4. We consider the same co-prime array and for each case, K equal strength sources are generated randomly in $[-65, 65]^\circ$, with $L = 20$ and SNR 20 dB. AP-GLS has higher estimation accuracy than CBF and estimating more sources than the number of sensors.

6. CONCLUSION

We introduced alternating projections based gridless sparse iterative covariance-based estimation for direction-of-arrival estimation that is gridless and promotes sparse solutions. Numerical evaluations indicated that the proposed method shows a favorable performance even with single-snapshot data and coherent arrivals. For co-prime array data, the proposed algorithm resolved more sources than the number of sensors.

7. REFERENCES

[1] D. Malioutov, M. Cetin, and A. S. Willsky, "A sparse signal reconstruction perspective for source localization with sensor arrays," *IEEE Trans. Signal Process.*, vol. 53, no. 8, pp. 3010–3022, Aug 2005.

[2] P. Gerstoft, A. Xenaki, and C.F. Mecklenbräuker, "Multiple and single snapshot compressive beamforming," *J. Acoust. Soc. Am.*, vol. 138, no. 4, pp. 2003–2014, 2015.

[3] A. Xenaki and P. Gerstoft, "Grid-free compressive beamforming," *J. Acoust. Soc. Am.*, vol. 137, no. 4, pp. 1923–1935, 2015.

[4] Y. Park, Y. Choo, and W. Seong, "Multiple snapshot grid free compressive beamforming," *J. Acoust. Soc. Am.*, vol. 143, no. 6, pp. 3849–3859, 2018.

[5] Z. Yang, J. Li, P. Stoica, and L. Xie, "Sparse methods for direction-of-arrival estimation," in *Academic Press Library in Signal Processing: Array, Radar and Communications Engineering*, vol. 7, chapter 11, pp. 509 – 581. Academic Press, 2018.

[6] G. Tang, B. N. Bhaskar, P. Shah, and B. Recht, "Compressed sensing off the grid," *IEEE Trans. Inf. Theory*, vol. 59, no. 11, pp. 7465–7490, 2013.

[7] Y. Chi, L. L. Scharf, A. Pezeshki, and A. R. Calderbank, "Sensitivity to basis mismatch in compressed sensing," *IEEE Trans. Signal Process.*, vol. 59, no. 5, pp. 2182–2195, 2011.

[8] Y. Chi and M. Ferreira Da Costa, "Harnessing sparsity over the continuum: Atomic norm minimization for superresolution," *IEEE Signal Process. Mag.*, vol. 37, no. 2, pp. 39–57, 2020.

[9] Y. Wang, Y. Zhang, Z. Tian, G. Leus, and G. Zhang, "Super-resolution channel estimation for arbitrary arrays in hybrid millimeter-wave massive MIMO systems," *IEEE J. Sel. Topics Signal Process.*, vol. 13, no. 5, pp. 947–960, Sep. 2019.

[10] A. G. Raj and J. H. McClellan, "Super-resolution DOA estimation for arbitrary array geometries using a single noisy snapshot," in *Proc. IEEE ICASSP*, 2019, pp. 4145–4149.

[11] S. Semper, F. Roemer, T. Hotz, and G. Del Galdo, "Grid-free direction-of-arrival estimation with compressed sensing and arbitrary antenna arrays," in *Proc. IEEE ICASSP*, 2018, pp. 3251–3255.

[12] Z. Yang, L. Xie, and C. Zhang, "A discretization-free sparse and parametric approach for linear array signal processing," *IEEE Trans. Signal Process.*, vol. 62, no. 19, pp. 4959–4973, 2014.

[13] P. Stoica, P. Babu, and J. Li, "SPICE: A sparse covariance-based estimation method for array processing," *IEEE Trans. Signal Process.*, vol. 59, no. 2, pp. 629–638, 2011.

[14] Z. Zhu and W. B. Wakin, "On the asymptotic equivalence of circulant and Toeplitz matrices," *IEEE Trans. Inf. Theory*, vol. 63, no. 5, pp. 2975–2992, 2017.

[15] D. Romero and G. Leus, "Wideband spectrum sensing from compressed measurements using spectral prior information," *IEEE Trans. Signal Process.*, vol. 61, no. 24, pp. 6232–6246, 2013.

[16] S. Boyd and L. Vandenberghe, *Convex optimization*, Cambridge university press, Cambridge, U.K., 2004.

[17] J. Dattorro, *Convex optimization & Euclidean distance geometry*, Meboo Publishing USA, Palo Alto, CA, USA, 2010.

[18] H. Q. Cai, J.-F. Cai, and K. Wei, "Accelerated alternating projections for robust principal component analysis," *J. Mach. Learn. Res.*, vol. 20, no. 1, pp. 685–717, 2019.

[19] X. Jiang, Z. Zhong, X. Liu, and H. C. So, "Robust matrix completion via alternating projection," *IEEE Signal Process. Lett.*, vol. 24, no. 5, pp. 579–583, 2017.

[20] A. S. Lewis and J. Malick, "Alternating projections on manifolds," *Math. Oper. Res.*, vol. 33, no. 1, pp. 216–234, 2008.

[21] P. Netrapalli, U. N. Niranjan, S. Sanghavi, A. Anandkumar, and P. Jain, "Non-convex robust PCA," in *Proc. NIPS*, 2014, pp. 1107–1115.

[22] M. Cho, J. Cai, S. Liu, Y. C. Eldar, and W. Xu, "Fast alternating projected gradient descent algorithms for recovering spectrally sparse signals," in *Proc. IEEE ICASSP*, 2016, pp. 4638–4642.

[23] L. Condat and A. Hirabayashi, "Cadzow denoising upgraded: A new projection method for the recovery of Dirac pulses from noisy linear measurements," *Sampl. Theory Signal Image Process.*, vol. 14, no. 1, pp. 17–47, 2015.

[24] X. Wu, W. Zhu, and J. Yan, "A Toeplitz covariance matrix reconstruction approach for direction-of-arrival estimation," *IEEE Trans. Veh.*, vol. 66, no. 9, pp. 8223–8237, Sep. 2017.

[25] M. Wagner, P. Gerstoft, and Y. Park, "Gridless DOA estimation via alternating projections," in *Proc. IEEE ICASSP*, 2019, pp. 4215–4219.

[26] M. Wagner, Y. Park, and P. Gerstoft, "Gridless DOA estimation and root-MUSIC for non-uniform arrays," *arXiv preprint arXiv:2003.04457*, 2020.

[27] P. P. Vaidyanathan and P. Pal, "Sparse sensing with co-prime samplers and arrays," *IEEE Trans. Signal Process.*, vol. 59, no. 2, pp. 573–586, 2010.

[28] S. Nannuru, A. Koochakzadeh, K. L. Gemba, P. Pal, and P. Gerstoft, "Sparse Bayesian learning for beamforming using sparse linear arrays," *J. Acoust. Soc. Am.*, vol. 144, no. 5, pp. 2719–2729, 2018.

[29] S. Nannuru, P. Gerstoft, A. Koochakzadeh, and P. Pal, "Sparse Bayesian learning for DOA estimation using co-prime and nested arrays," in *Proc. 10th IEEE SAM*, 2018, pp. 519–523.

[30] C. Steffens, M. Pesavento, and M. E. Pfetsch, "A compact formulation for the $\ell_{2,1}$ mixed-norm minimization problem," *IEEE Trans. Signal Process.*, vol. 66, no. 6, pp. 1483–1497, 2018.

[31] M. G. Eberle and M. C. Maciel, "Finding the closest Toeplitz matrix," *Comput. Appl. Math.*, vol. 22, no. 1, pp. 1–18, 2003.

[32] P. Stoica and A. Nehorai, "Music, maximum likelihood, and Cramér-Rao bound," *IEEE Trans. Acoust., Speech, Signal Process.*, vol. 37, no. 5, pp. 720–741, 1989.

[33] C. Liu and P. P. Vaidyanathan, "Remarks on the spatial smoothing step in coarray MUSIC," *IEEE Signal Process. Lett.*, vol. 22, no. 9, pp. 1438–1442, 2015.